


Homogeneous crystallization in four-dimensional Lennard-Jones liquidsRobert S. Hoy *Department of Physics, University of South Florida, Tampa, Florida 33620, USA*

(Received 6 November 2023; accepted 25 March 2024; published 15 April 2024)

We observe homogeneous crystallization in simulated high-dimensional ($d > 3$) liquids that follow physically realistic dynamics and have system sizes that are large enough to eliminate the possibility that crystallization was induced by the periodic boundary conditions. Supercooled four-dimensional (4D) Lennard-Jones (LJ) liquids maintained at zero pressure and constant temperatures $0.59 < T < 0.63$ crystallized within $\sim 2 \times 10^4 \tau$, where τ is the LJ time unit. Weeks-Chandler-Andersen (WCA) liquids that were maintained at the same densities and temperatures at which their LJ counterparts nucleated did not crystallize even after $2.5 \times 10^5 \tau$, showing that the presence of long-ranged attractive interactions dramatically speeds up 4D crystallization, much as it does in 3D. On the other hand, the overlap of the liquid and crystalline phases' local-bond-order distributions is smaller for LJ systems than for WCA systems, which is the opposite of the 3D trend. This implies that the widely accepted hypothesis that increasing geometrical frustration rapidly suppresses crystallization as the spatial dimension d increases is only generally valid in the absence of attractive interparticle forces.

DOI: [10.1103/PhysRevE.109.044604](https://doi.org/10.1103/PhysRevE.109.044604)**I. INTRODUCTION**

In three-dimensional liquids composed of monodisperse particles lacking strongly directional interactions, local structural ordering at the atomic scale is typically approximately icosahedral [1]. Icosahedra, which are composed of a central atom surrounded by 12 atoms that form a locally fivefold-symmetric shell, are the lowest-energy 13-atom structures for a wide range of pair potentials [2]; they are composed of 20 distinct tetrahedra, which are the lowest-energy 4-atom structures. Both tetrahedra and icosahedra, however, are incompatible with these potentials' lowest-energy *global* structures, i.e., with the fcc and hcp crystal lattices. Such incompatibility between the lowest-energy *local* structures and the lowest-energy *global* structures is known as “geometrical frustration” and is one of the best-known reasons for glass formation [3]. It makes the free energy barriers for rearrangements from locally into globally preferred structures large, increases atoms' tendency to stay in the former under rapid cooling or compression, and promotes the formation of locally polytetrahedral amorphous order at the expense of close-packed crystalline order in a wide variety of 3D glassy and jammed solids [4].

Three-dimensional systems are, however, somewhat unusual in this respect. In two dimensions, the lowest-energy 7-atom clusters (for the same pair potentials that give icosahedra in 3D) are hexagons composed of 6 triangles, which are the lowest-energy 3-atom structures. Since these structures are both compatible with the triangular lattice, monodisperse 2D soft-sphere and hard-sphere liquids readily crystallize [5] under a wide range of preparation protocols [7–10]. In four dimensions, the lowest-energy/most-compact 25-atom

clusters are composed of 24 octahedral cells, which are the lowest-energy/most-compact 8-atom structures. Both of these structures are compatible with the D_4 lattice, which is the densest 4D sphere packing [11]. Thus it was surprising to find that crystallization of 4D hard-sphere liquids is strongly suppressed. In the first study of these liquids' solidification dynamics [12], crystallization occurred in a very slowly compressed, very small (648-atom) system, but none was observed in a 10 000-atom system, suggesting that the 648-atom result may have been a finite-size artifact arising from the periodic boundary conditions [13]. More recent studies of larger systems also failed to observe homogeneous crystallization [14–22].

van Meel *et al.* explained this failure in terms of a less-obvious kind of geometrical frustration, namely, that the *actual* local ordering in equilibrated 4D hard-sphere liquids is very different than that of the abovementioned 25-atom clusters [14,15]. More specifically, the overlap \mathcal{O} of the probability distributions for local bond order (q_6 [23]) in the metastable supercooled liquid and equilibrium crystalline states,

$$\mathcal{O} = \int_0^1 P_{\text{liquid}}(q_6) P_{\text{cryst}}(q_6) dq_6, \quad (1)$$

is far smaller in 4D than it is in 3D, and consequently the free energy barriers to crystal nucleation (and specifically, the interfacial free energy) are much higher. This type of entropically driven frustration gets more dramatic as the spatial dimension d increases [15], consistent with the now-widely-accepted notion that crystallization rapidly gets harder with increasing d [12]. Its presence can explain why crystallization is suppressed in high d despite the fact that systems' equilibrium freezing densities remain well below their glass transition densities [19,20].

*rshoy@usf.edu

On the other hand, there are reasons to question whether results for hard-sphere liquids can be generalized to other systems. While the structure of liquids at the level of the pair correlation function $g(r)$ is determined almost completely by the repulsive-core part of the interatomic interactions (for systems maintained at fixed density ρ and temperature T [24]), longer-ranged attractive forces can exert a substantial influence on higher-order structural metrics that influence crystallization propensity [25]. Toxvaerd recently showed [26] that increasing the potential cutoff radius r_c in 3D Lennard-Jones (LJ) liquids from its Weeks-Chandler-Andersen value ($r_c^{\text{WCA}} = 2^{1/6}\sigma$, where σ is the LJ length unit) to 3.5σ (a value that produces attractive forces for particles in atoms' first, second, and third coordination shells) increased both their \mathcal{O} values and their nucleation rates by at least 1 order of magnitude. This result leads naturally to the question: is the same combination of trends also present in higher d ?

Higher- d liquids are, of course, not experimentally realizable, but studying them can reveal which factors are most important in controlling the physics of realizable ($d \leq 3$) systems, especially for phenomena (e.g., solidification) that are markedly different in 2D vs 3D [27]. However, to the best of our knowledge, only three previously published particle-based simulation studies of $d > 3$ liquids have included attractive interactions [28–30], and none of these examined systems that could be expected to crystallize. Here, using large-scale molecular dynamics simulations of 4D WCA and Lennard-Jones liquids, we show that the answer to the above question is, surprisingly, no. LJ liquids reproducibly nucleate and form high-quality D_4 crystals over times as small as $\sim 10^4\tau$, at densities and temperatures for which WCA liquids do not crystallize on any currently computationally-feasible time scale. This difference occurs despite the fact that the LJ systems have \mathcal{O} values that are slightly *lower* than their WCA counterparts. Our results imply that the widely accepted hypothesis that increasing geometrical frustration rapidly suppresses crystallization as the spatial dimension d increases is only generally valid *in the absence of attractive interparticle forces*.

II. METHODS

All simulations were performed using hdMD [31]. Systems are composed of $N = 5 \times 10^5$ particles of mass m , interacting via the truncated and shifted Lennard-Jones potential $U_{\text{LJ}}(r) = 4\epsilon[(\sigma/r)^{12} - (\sigma/r)^6 - (\sigma/r_c)^{12} + (\sigma/r_c)^6]$, where ϵ is the interparticle binding energy and r_c is the cutoff radius. Newton's equations of motion are integrated with a time step of $dt = \tau/125$, where $\tau = \sqrt{m\sigma^2/\epsilon}$ is the LJ time unit. Periodic boundary conditions are applied along all four directions of hypercubic simulation cells. After initially placing the particles randomly within the cells and minimizing their energy to reduce interparticle overlap, short NVT-ensemble equilibration runs are performed. For the LJ ($r_c = r_c^{\text{LJ}} \equiv 2.5\sigma$) systems, these are followed by long NPT-ensemble runs of lengths up to $10^5\tau$, where pressure is maintained at zero and temperature is held constant using a Berendsen thermostat/barostat [32]. In the later stages of our study, we also performed NVT simulations of WCA ($r_c = r_c^{\text{WCA}} \equiv 2^{1/6}\sigma$) liquids and both LJ and WCA D_4 single

crystals; these are described further in Sec. III. Below, we express all quantities in dimensionless (LJ) units.

In addition to standard thermodynamic metrics such as the average pair interaction energy per particle E_{pair} , the particle number density ρ , and the pair correlation function $g(r)$, we monitor two structural order parameters that have been shown to effectively characterize the types of 4D crystallization we might expect to encounter [14,15]: specifically, the second-order two-particle bond-order correlators $q_4(i, j)$ and $q_6(i, j)$, where

$$q_l(i, j) = \frac{1}{\mathcal{N}(i)\mathcal{N}(j)} \sum_{\alpha=1}^{\mathcal{N}(i)} \sum_{\beta=1}^{\mathcal{N}(j)} G_l^1(\hat{r}_{i\alpha} \cdot \hat{r}_{j\beta}). \quad (2)$$

Here G_l^1 are Gegenbauer polynomials defined by [33]

$$G_l^1(x) = \sum_{k=0}^{l/2} \frac{(-1)^k (l-k)! (2x)^{l-2k}}{k! (l-2k)!}. \quad (3)$$

We calculate $q_4(i, j)$ and $q_6(i, j)$ for all neighboring particles i and j that lie within each other's first coordination shells as defined by the first minimum of $g(r)$, i.e., all particle pairs (i, j) whose distance $r_{ij} = |\vec{r}_j - \vec{r}_i| < 1.4$. The sums in Eq. (2) are performed over the $\mathcal{N}(i)$ neighbors of particle i and $\mathcal{N}(j)$ neighbors of particle j satisfying $r_{i\alpha}, r_{j\beta} < 1.4$. These rotationally invariant correlators are defined so that $q_4(i, j) = 1$ [$q_6(i, j) = 1$] in perfect A_4 [D_4] lattices [11] and both $|q_l(i, j)| \ll 1$ in a liquid; see Ref. [15] for a detailed discussion. We also monitor the per-particle quantities $\tilde{q}_l(i)$ defined by averaging these $q_l(i, j)$ over all neighbors of particle i :

$$\tilde{q}_l(i) = \frac{1}{\mathcal{N}(i)} \sum_{j=1}^{\mathcal{N}(i)} q_l(i, j). \quad (4)$$

Recent work has demonstrated that even for single-component systems with central-force interactions, crystallization typically involves nontrivially correlated fluctuations of at least two order parameters (OPs) associated with translational and rotational symmetry breaking, and that properly understanding crystallization requires examining both types of OPs [34,35]. In particular, fluctuations in local density and local orientational order both tend to trigger nucleation, but which type of fluctuation is more likely to do so is system dependent [36,37]. Thus, we also monitor the local packing fraction

$$\phi_{\text{loc}}(i) = \frac{V_{\text{pis}}(i)}{V_{\text{is}}}, \quad (5)$$

where $V_{\text{is}} = \pi^2 (r_c^{\text{LJ}})^4 / 32$ is the volume of a hyperspherical shell of radius r_c^{LJ} , and $V_{\text{pis}}(i)$ is the total particle volume lying within the shell centered on particle i . We calculated $V_{\text{pis}}(i)$ accurately using Li's method for determining the intersection volume of two overlapping hyperspheres [38]. For the purposes of this calculation, particles were treated as hyperspheres of diameter $2^{1/6}$, i.e., of diameter equal to the interparticle distance at which both LJ and WCA forces vanish.

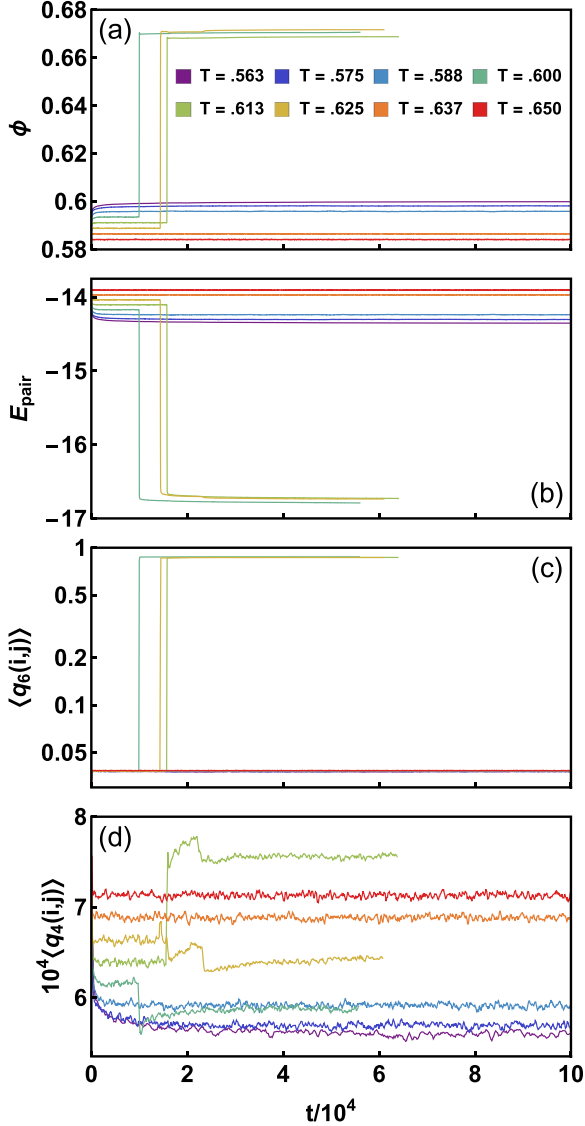


FIG. 1. Average packing fraction $\phi \equiv \rho V_{\text{is}}$, average pair energy E_{pair} , and average two-particle bond-order correlators $\langle q_6(i, j) \rangle$ and $\langle q_4(i, j) \rangle$ in supercooled 4D Lennard-Jones liquids maintained at zero pressure and the temperatures indicated in the legend of panel (a).

III. RESULTS

Figure 1 illustrates the evolution of four structural metrics at eight different temperatures over the range $0.5625 \leq T \leq 0.650$. In all systems with $0.600 \leq T \leq 0.625$, E_{pair} drops sharply while ϕ and $\langle q_6(i, j) \rangle$ increase sharply at various $t < 2 \times 10^4$; here t is the time elapsed since the beginning of the NPT runs, and the average is taken over all $(i, j) \in [1, N]$. The combination of high final $\langle q_6(i, j) \rangle$ values with low final $\langle q_4(i, j) \rangle$ values indicates that these systems have crystallized into the D_4 rather than the competing (A_4) crystal structure [15].

In systems with lower and higher T , no such rapid changes in any of these quantities occur. Since fast crystallization of large systems requires both rapid nucleation and rapid growth, we expect that $0.59 \lesssim T \lesssim 0.63$ is, roughly

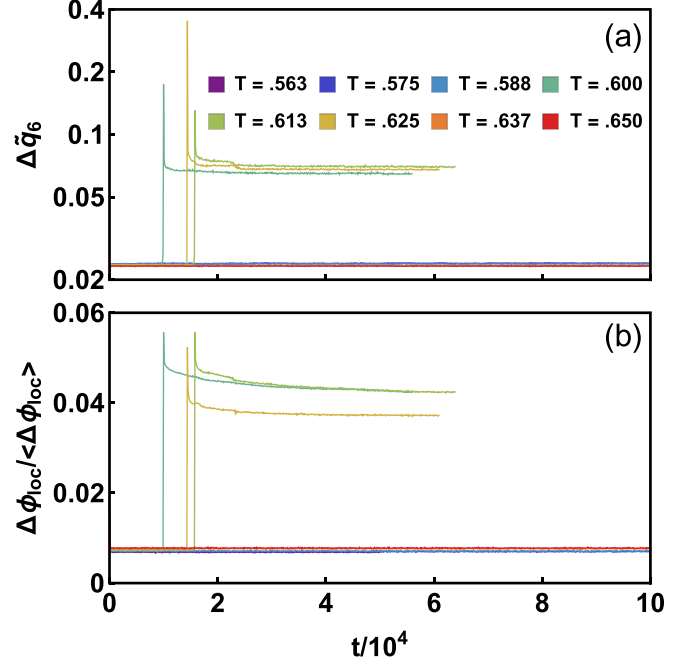


FIG. 2. Fluctuations in the per-particle bond-order correlator $\tilde{q}_6(i)$ and the local packing fraction $\phi_{\text{loc}}(i)$ in supercooled 4D Lennard-Jones liquids maintained at zero pressure and the temperatures indicated in the legend of panel (a).

speaking, the range where both nucleation and growth rates are large (see, e.g., Fig. 3 of Ref. [39]). The apparent absence of crystallization for $T < 0.6$ is probably an artifact of the finite observation window ($\Delta t = 10^5$), but it seems unlikely that it results from these liquids failing to equilibrate; note that the rms particle displacements over this window were at least four particle diameters even for the lowest $T = 0.5625$.

The first-order-transition-like jumps in ϕ and $\langle q_6(i, j) \rangle$ for $0.600 \leq T \leq 0.625$ are accompanied by massive local fluctuations in the corresponding single-particle quantities. Figure 2 shows that $\Delta \tilde{q}_6 = [(\tilde{q}_6(i)^2) - \langle \tilde{q}_6(i)^2 \rangle]^{1/2}$ and $\Delta \phi_{\text{loc}} = [(\phi_{\text{loc}}(i)^2) - \langle \phi_{\text{loc}}(i)^2 \rangle]^{1/2}$ exhibit sharp maxima coinciding with these jumps. Both quantities increase by roughly an order of magnitude for a very short time interval ($< 10^2$ LJ time units) before rapidly dropping back to intermediate values and then finally slowly decreasing for larger t . It is unclear whether $\Delta \tilde{q}_6$ or $\Delta \phi_{\text{loc}}$ is maximized first, raising a question that has been recently investigated for 3D liquids [35,37,40]: do orientational-order fluctuations trigger positional-order (i.e., density) fluctuations or vice versa? We examine this question in more detail below.

Next we examine how the *distributions* of positional and orientational order evolve. Results for a single representative temperature ($T = 0.625$) are shown in Fig. 3. Panel (a) focuses on the pair correlation function $g(r)$. At $t = 1.40 \times 10^4$ and 1.43×10^4 , $g(r)$ takes a typical liquid-state form. At $t = 1.44 \times 10^4$, the system is evidently in an intermediate state containing (unstable) coexisting liquid and crystalline regions. At $t = 1.45 \times 10^4$ and all later times, e.g., $t = 5.00 \times 10^4$ as shown in the plot, the system has solidified into a high-quality crystal. We verified that it is, in fact, a D_4 crystal by checking that the coordination number

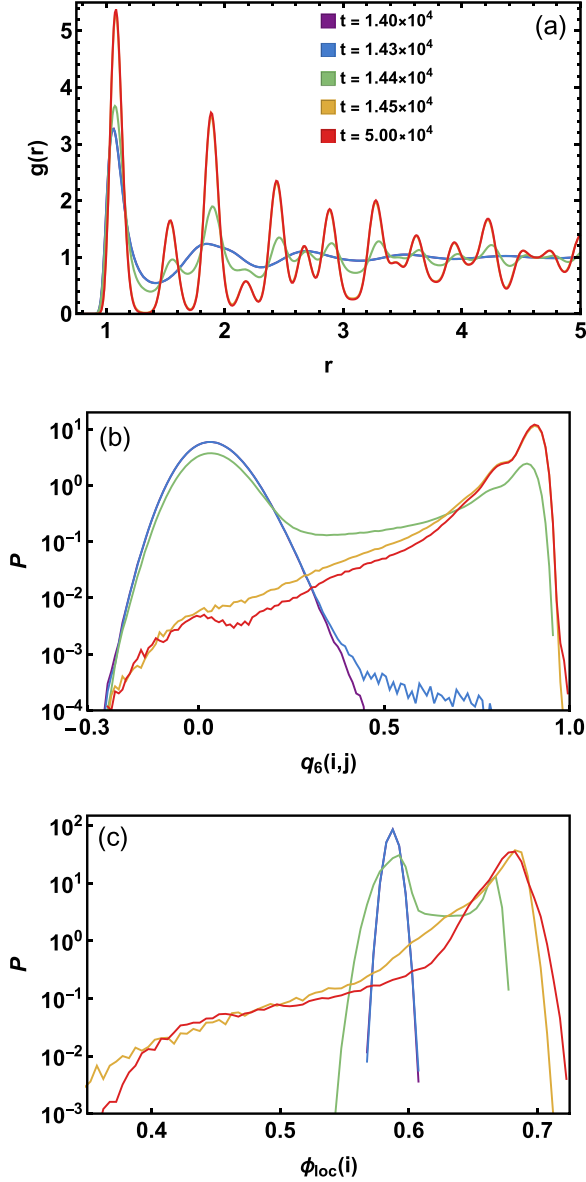


FIG. 3. Evolution of local structural order in Lennard-Jones systems at $T = 0.625$ and $P = 0$. Panels (a)–(c) respectively show the pair correlation functions $g(r)$, the probability distributions $P[q_6(i, j)]$, and the probability distributions $P[\phi_{\text{loc}}(i)]$ at selected times.

$Z = \int_0^{1.4} 2\pi^2 \rho r^3 g(r) dr$ [the 4D analogue of the familiar 3D formula $Z = \int_0^{1.4} 4\pi \rho r^2 g(r) dr$] is close to 24; indeed, $Z \simeq 23.81$ at $t = 1.45 \times 10^4$ and thereafter continues increasing slowly with t .

As expected from the decorrelation principle [12,41], the secondary and tertiary peaks of the liquid-state $g(r)$ are slightly less sharp than in a comparable metastable 3D liquid [26]. On the other hand, as expected from previous studies of four-, five-, and six-dimensional hard-sphere systems [21,42], the coordination shells of the D_4 crystal are much more sharply defined those of the corresponding 3D crystal. For example, if r_{max} and r_{min} correspond to the first maximum and minimum of $g(r)$, the D_4 crystal has

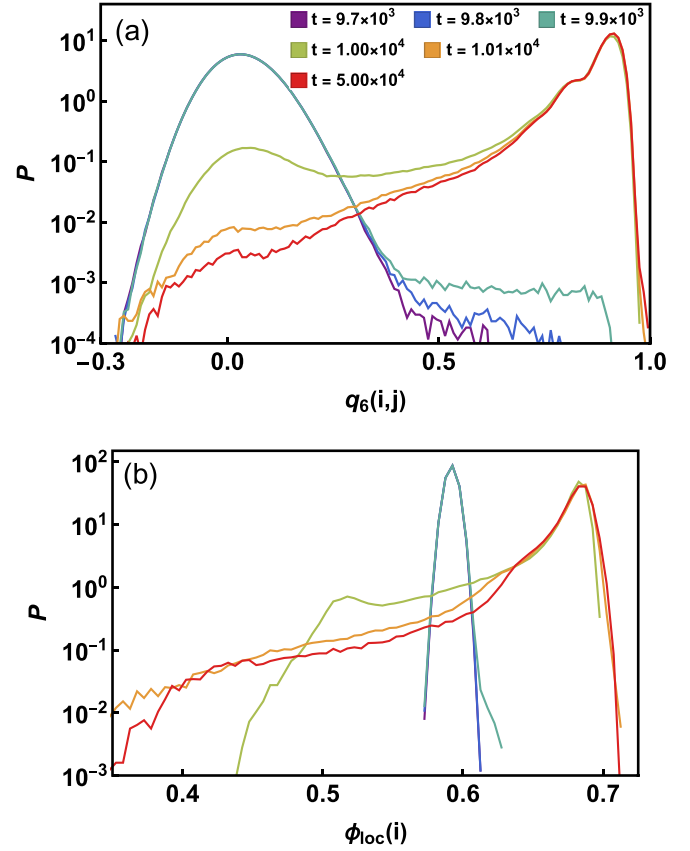


FIG. 4. Evolution of local structural order in Lennard-Jones systems at $T = 0.600$ and $P = 0$. Panels (a) and (b) respectively show the probability distributions $P[q_6(i, j)]$ and the probability distributions $P[\phi_{\text{loc}}(i)]$ at selected times.

$g(r_{\text{max}}) \simeq 5.5$ and $g(r_{\text{min}}) \simeq 0.013$, whereas a comparable fcc crystal has $g(r_{\text{max}}) \simeq 4$ and $g(r_{\text{min}}) \simeq 0.2$ [26]. This combination of less-correlated liquid structure and more-correlated crystal structure substantially increases entropic contributions to the free energy barriers for crystal nucleation [12,14,15,18,21].

Further insights can be obtained by looking at the probability distributions for $q_6(i, j)$ and $\phi_{\text{loc}}(i)$ [Figures 3(b) and 3(c)]. Crystal nucleation is indicated by the appearance of a high- q_6 tail in $P[q_6(i, j)]$ at $t = 1.43 \times 10^4$. At this point, the local bond order in the system is $\sim 0.014\%$ crystalline as measured by the fraction of (i, j) pairs that have $q_6(i, j) \geq 0.4$ [14]. This fraction grows to $\sim 33\%$ over the next 100τ , and by $t = 1.45 \times 10^4$ it is 99.2% . Thereafter it continues growing slowly. Notably, at $t = 1.43 \times 10^4$, there is as of yet no high- ϕ_{loc} tail in $P[\phi_{\text{loc}}(i)]$ to match the abovementioned high- q_6 tail in $P[q_6(i, j)]$. Also note that the long low- q_6 tails in $P[q_6(i, j)]$ for $t \geq 1.45 \times 10^4$ are matched by long low- ϕ_{loc} tails in $P[\phi_{\text{loc}}(i)]$, indicating that those parts of the system which remain poorly crystallized contain voids that may eventually anneal out. As shown in Fig. 4, the same sequence (appearance of a high- q_6 tail in $P[q_6(i, j)]$) followed shortly thereafter by the appearance of a high- ϕ_{loc} tail in $P[\phi_{\text{loc}}(i)]$) is observed for $T = 0.600$; this sequence also occurs for $T = 0.613$. These results suggest that orientational-order fluctuations often trigger positional-order (i.e., density) fluctuations

TABLE I. Particle number densities employed in the NVT WCA simulations.

T	ρ	T	ρ
0.5625	1.226	0.6125	1.207
0.575	1.222	0.625	1.202
0.5875	1.217	0.6375	1.198
0.600	1.212	0.650	1.193

in 4D LJ liquids, much as they have been shown to do in 3D hard-sphere and LJ liquids [37,40].

All of these systems had periodic simulation cell side lengths $L \gtrsim 25\sigma$ for all t , removing the possibility that crystallization was promoted by the periodic boundary conditions as may have been the case [13] for the 648-atom systems studied in Ref. [12]. Performing these simulations was enabled by hdMD's efficient parallel implementation, which allowed us to perform simulations with an N (5×10^5) that was at least ten times larger than those employed in any previous $d > 3$ simulations other than those of Ref. [31]. On the other hand, the drawback to employing such a large N was that limited computational resources prevented us from simulating multiple independently prepared systems at the same state point, as is typically done in modern simulation studies to obtain robust results for any stochastic process (e.g., crystallization [26,37]). Since orientational-order fluctuations consistently appear slightly *before* density fluctuations (Figs. 3 and 4), it seems unlikely that simulating these liquids in NVT (as opposed to NPT) ensembles would qualitatively change their crystal-*nucleation* dynamics. Employing NVT ensembles could have a larger effect on the crystal-*growth* dynamics since it would suppress ϕ_{loc} fluctuations, but since this is not our main focus, we defer examination of this possibility to future work, and turn our attention to how the key results discussed above are affected by the choice of interparticle interactions (LJ or WCA) for a wide range of T .

To better understand the role played by attractive forces [43], we followed the strategy employed in Ref. [26] and performed NVT runs of length $2.5 \times 10^5 \tau$ for WCA liquids at each of the eight T values highlighted in Figs. 1 and 2. Runs were conducted either at the ρ values the corresponding LJ liquids had just before they crystallized (for $T = 0.600, 0.613$, and 0.625) or at the ρ values the noncrystallizing systems reached in the large- t limit; numerical values are given in Table I. None of these liquids showed any signs of crystallization. In particular, as shown in Fig. 5, the pressure, $\langle q_6(i, j) \rangle$, and $\Delta\phi_{\text{loc}}/\langle\phi_{\text{loc}}\rangle$ all remained stable for all eight T , despite the fact that the reduced pressures $\tilde{p} = p/(\rho k_B T)$ were more than double the equilibrium liquid-crystal coexistence pressure $\tilde{p}_{\text{coex}} = 10.8$ [19]. This result is consistent with previous studies of 4D hard-sphere liquids [14–21].

Why, then, do 4D Lennard-Jones liquids readily form high-quality crystals when hard-sphere and WCA liquids do not? In an attempt to gain further insight, we compared the time-averaged E_{pair} and $P[q_6(i, j)]$ for LJ and WCA liquids and D_4 single crystals at the same temperatures and densities, for the three T for which the LJ liquids crystallized at $t \sim 10^4$ [45]. The single-crystal systems were prepared using NVT

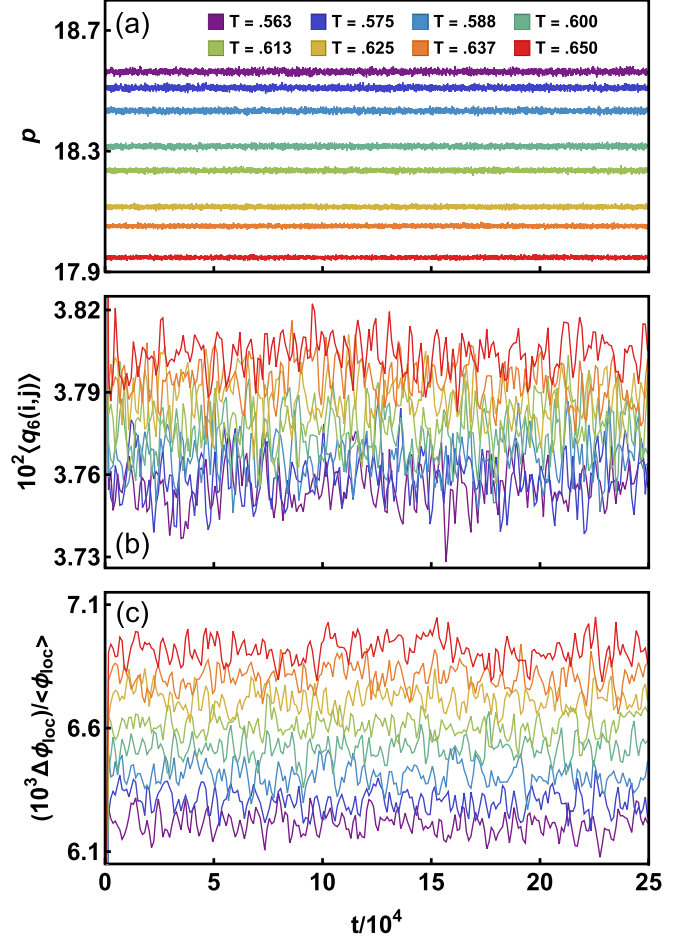


FIG. 5. Pressure p , average two-particle bond-order correlator $\langle q_6(i, j) \rangle$, and average fractional density fluctuations $\Delta\phi_{\text{loc}}/\langle\phi_{\text{loc}}\rangle$ in supercooled 4D WCA liquids maintained at constant densities and temperatures (Table I).

equilibration runs at the densities these LJ systems reached in the limit $t \rightarrow \infty$ [Fig. 1(a)], e.g., $\rho = 1.372$ for $T = 0.625$. Results are summarized in Fig. 6 and Table II. Figure 6(a) shows that the LJ liquids' $P[q_6(i, j)]$ have slightly longer high- q_6 tails compared to those of the WCA liquids, while the WCA crystals' $P[q_6(i, j)]$ have *much* longer low- q_6 tails compared to those of the LJ crystals. As a consequence, \mathcal{O} [Eq. (1)] is slightly larger for the WCA systems than it is for the LJ systems [46]. Examining positional rather than orientational order yields an analogous trend. Figure 6(b) shows

TABLE II. $\Delta E_{\text{pair}} = E_{\text{pair}}^{\text{cryst}} - E_{\text{pair}}^{\text{liquid}}$ and \mathcal{O} for the three T for which LJ liquids crystallized [45].

Potential	T	ΔE_{pair}	\mathcal{O}
WCA	0.600	-0.166	6.1×10^{-9}
	0.613	-0.181	3.7×10^{-9}
	0.625	-0.231	3.3×10^{-9}
LJ	0.600	-2.75	4.8×10^{-9}
	0.613	-2.81	2.5×10^{-9}
	0.625	-2.87	1.5×10^{-9}

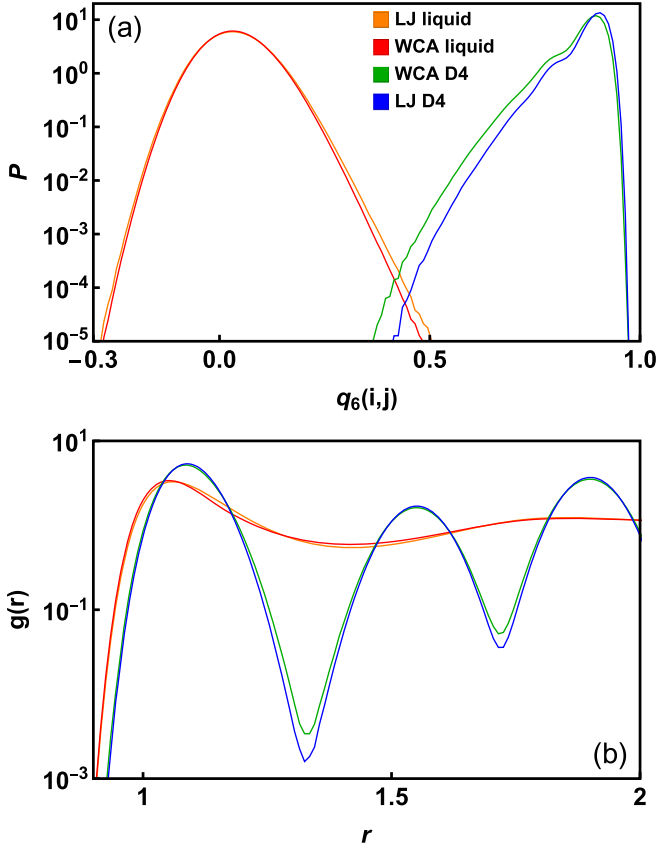


FIG. 6. Time-averaged results for $P[q_6(i, j)]$ [panel (a)] and $g(r)$ [panel (b)] in LJ and WCA liquids at the same $\rho = 1.202$ and LJ and WCA single D_4 crystals at the same $\rho = 1.372$.

that the liquid and crystalline $g(r)$ are slightly more similar in WCA than in LJ systems; in particular, WCA crystals have a larger $g(r_{\min})$. All the available data suggest that WCA systems have a surface tension smaller than that of their LJ counterparts [14,15].

Larger \mathcal{O} lower the entropic barriers to crystallization by increasing the likelihood for localized regions within a supercooled liquid to have crystal-like bond order [40]. This was cited as the primary reason why 3D LJ systems crystallize much faster than their WCA counterparts [26]. In 4D, however, it appears that the small differences in \mathcal{O} are easily overcome by the large differences in ΔE_{pair} . In other words, it appears that energy trumps entropy in determining how rapidly these systems crystallize. This effect cannot be captured by the hard-sphere models employed in all previous studies of crystallization (or the lack thereof) in $d > 3$ [12,14–21] because such systems' potential energies are identically zero.

IV. DISCUSSION AND CONCLUSIONS

References [14,15] showed that the absence of the most obvious type of geometrical frustration, namely, the incompatibility of the lowest-energy/maximally dense local structure with the ground-state crystal, does not mean that supercooled 4D hard-sphere liquids can easily crystallize. This is true because the *actual* local structure of these liquids is very

different than their maximally dense local structure. The overlap \mathcal{O} [Eq. (1)] of local bond order distributions in the supercooled-liquid and equilibrium-crystalline states is surprisingly (and substantially) less in 4D than it is in 3D, and it continues to decrease rapidly, leading to free energy barriers to crystallization that grow rapidly, with increasing d [14,15]. This trend is consistent with the recent observation that increasing r_c in 3D WCA and LJ systems substantially increases both their \mathcal{O} values and their nucleation rates [26].

Here we showed that 4D WCA and LJ systems violate this paradigm. Specifically, we showed that supercooled $N = 5 \times 10^5$ LJ liquids maintained at zero pressure and constant temperatures $0.59 < T < 0.63$ formed high-quality D_4 crystals within $\sim 2 \times 10^4 \tau$, whereas WCA liquids that were maintained at the same densities and temperatures at which their LJ counterparts nucleated did not crystallize even after $2.5 \times 10^5 \tau$, despite the fact that the WCA systems had slightly larger \mathcal{O} values. One would expect that the LJ systems' much larger $-\Delta E_{\text{pair}}$ (Table II) would dramatically speed up their crystallization, but ours was (to the best of our knowledge) the first actual observation of homogeneous crystallization in simulated $d > 3$ liquids that followed physical (Newtonian) dynamics [22] and were large enough to eliminate the possibility that crystallization was promoted by the periodic boundary conditions.

Since $-\Delta E_{\text{pair}}$ in systems with at-least-intermediate-range attractive interactions probably continues to grow with d [19,21,42], our results suggest that the widely accepted hypothesis that crystallization rapidly gets harder with increasing d [12,14,15] is only generally valid *in the absence of attractive interactions*. At the very least, when considered in combination with our demonstration that higher \mathcal{O} values do not necessarily lead to higher nucleation rates, they suggest that accounting for energetic (not just entropic) contributions to the free energy barriers to crystallization is necessary to determine whether this hypothesis is true in general.

Here we compared LJ systems to WCA systems at the same ρ and T . This strategy is commonly employed in studies of how attractive forces influence crystallization because it allows comparison of systems with similar liquid-state $g(r)$ [26], but it leaves several fundamental questions open. For example, how strongly do the results discussed above depend on the applied pressure? At the pressure employed in this study ($p = 0$), attractive and repulsive forces in the LJ systems are roughly equally important. As p increases, however, repulsive forces should increasingly dominate [24], and both LJ and WCA systems' solidification behavior should gradually approach the same hard-sphere-limit behavior as $p \rightarrow \infty$. Examining how this crossover occurs could improve the comparability of our results to experiments, which are typically conducted at fixed p and T [35].

Moreover, systems at the same ρ and T will, in general, have different degrees of supercooling, i.e., different T/T_{melt} , where T_{melt} is the equilibrium melting temperature. Comparing systems at the same T/T_{melt} could determine to what extent the much faster crystallization of LJ systems reported above arises from deeper supercooling, especially if this comparison were combined with studying how their interfacial free energies, chemical potential differences, and critical-nucleus radii depend on T [15,35]. However, since performing

these investigations would require carrying out very extensive (and very computationally expensive) additional simulations and data analyses, we leave these questions to future work.

We conclude by mentioning one additional potential implication of our results for future studies of the glass transition. Monodisperse 4D hard-sphere and repulsive soft-sphere liquids are particularly useful for studies of this transition [16,18,47,48] because they lack the strong correlations between particle size and particle mobility which make it challenging to interpret the heterogeneous dynamics of model

bidisperse and polydisperse supercooled liquids [49–51]. Our results demonstrate another way such liquids can be useful: their crystallization propensity can be tuned by varying their cutoff radius r_c .

ACKNOWLEDGMENTS

We thank Patrick Charbonneau for helpful discussions. This material is based upon work supported by the National Science Foundation under Grant No. DMR-2026271.

-
- [1] F. C. Frank, Supercooling of liquids, *Proc. R. Soc. London A* **215**, 43 (1952).
 - [2] J. P. K. Doye and D. J. Wales, The effect of the range of the potential on the structures of clusters, *J. Chem. Phys.* **103**, 4234 (1995).
 - [3] D. R. Nelson, Order, frustration, and defects in liquids and glasses, *Phys. Rev. B* **28**, 5515 (1983).
 - [4] A. V. Anikeenko and N. N. Medvedev, Polytetrahedral nature of the dense disordered packings of hard spheres, *Phys. Rev. Lett.* **98**, 235504 (2007).
 - [5] Albeit in such a way that they form at most *quasi*-long-range order; true 2D crystalline order is thermodynamically forbidden [6].
 - [6] N. D. Mermin, Crystalline order in two dimensions, *Phys. Rev.* **176**, 250 (1968).
 - [7] P. Pieranski, Two-dimensional interfacial colloidal crystals, *Phys. Rev. Lett.* **45**, 569 (1980).
 - [8] B. D. Lubachevsky, F. H. Stillinger, and E. N. Pinson, Disks vs spheres: Contrasting properties of random packings, *J. Stat. Phys.* **64**, 501 (1991).
 - [9] P. M. Reis, R. A. Ingale, and M. D. Shattuck, Crystallization of a quasi-two-dimensional granular fluid, *Phys. Rev. Lett.* **96**, 258001 (2006).
 - [10] A. E. González, Colloidal crystallization in 2D for short-ranged attractions: A descriptive overview, *Crystals* **6**, 46 (2016).
 - [11] J. H. Conway and N. J. A. Sloane, *Sphere Packings, Lattices and Groups*, 2nd ed., Grundlehren der Mathematischen Wissenschaften (Springer-Verlag, New York, 1993).
 - [12] M. Skoge, A. Donev, F. H. Stillinger, and S. Torquato, Packing hyperspheres in high-dimensional Euclidean spaces, *Phys. Rev. E* **74**, 041127 (2006).
 - [13] Since the D_4 lattice has eight atoms per unit cell [11], the choice $N = 648$ promotes the formation of a $3 \times 3 \times 3 \times 3$ -cell D_4 single crystal.
 - [14] J. A. van Meel, D. Frenkel, and P. Charbonneau, Geometrical frustration: A study of four-dimensional hard spheres, *Phys. Rev. E* **79**, 030201(R) (2009).
 - [15] J. A. van Meel, B. Charbonneau, A. Fortini, and P. Charbonneau, Hard-sphere crystallization gets rarer with increasing dimension, *Phys. Rev. E* **80**, 061110 (2009).
 - [16] P. Charbonneau, A. Ikeda, J. A. van Meel, and K. Miyazaki, Numerical and theoretical study of a monodisperse hard-sphere glass former, *Phys. Rev. E* **81**, 040501(R) (2010).
 - [17] P. Charbonneau, A. Ikeda, G. Parisi, and F. Zamponi, Dimensional study of the caging order parameter at the glass transition, *Proc. Natl. Acad. Sci. USA* **109**, 13939 (2012).
 - [18] B. Charbonneau, P. Charbonneau, and G. Tarjus, Geometrical frustration and static correlations in hard-sphere glass formers, *J. Chem. Phys.* **138**, 12A515 (2013).
 - [19] P. Charbonneau, C. M. Gish, R. S. Hoy, and P. K. Morse, Thermodynamic stability of hard sphere crystals in dimensions 3 through 10, *Eur. Phys. J. E* **44**, 101 (2021).
 - [20] P. Charbonneau, P. K. Morse, W. Perkins, and F. Zamponi, Three simple scenarios for high-dimensional sphere packings, *Phys. Rev. E* **104**, 064612 (2021).
 - [21] L. Lue, M. Bishop, and P. A. Whitlock, The fluid to solid phase transition of hard hyperspheres in four and five dimensions, *J. Chem. Phys.* **132**, 104509 (2010).
 - [22] Homogeneous crystallization of larger 4D hard-sphere liquids has been induced using a configurational-bias Monte Carlo method [14,15], but it has not yet been reported in systems following the normal physical dynamics.
 - [23] P. J. Steinhardt, D. R. Nelson, and M. Ronchetti, Bond-orientational order in liquids and glasses, *Phys. Rev. B* **28**, 784 (1983).
 - [24] J. D. Weeks, D. Chandler, and H. C. Andersen, Role of repulsive forces in determining equilibrium structure of simple liquids, *J. Chem. Phys.* **54**, 5237 (1971).
 - [25] J. Taffs, A. Malins, S. R. Williams, and C. P. Royall, The effect of attractions on the local structure of liquids and colloidal fluids, *J. Chem. Phys.* **133**, 244901 (2010).
 - [26] S. Toxvaerd, Role of the attractive forces in a supercooled liquid, *Phys. Rev. E* **103**, 022611 (2021).
 - [27] D. R. Nelson and B. I. Halperin, Dislocation-mediated melting in two dimensions, *Phys. Rev. B* **19**, 2457 (1979).
 - [28] M. Hloucha and S. I. Sandler, Phase diagram of the four-dimensional Lennard-Jones fluid, *J. Chem. Phys.* **111**, 8043 (1999).
 - [29] R. Brüning, D. A. St-Onge, S. Patterson, and W. Kob, Glass transitions in one-, two-, three-, and four-dimensional binary Lennard-Jones systems, *J. Phys.: Condens. Matter* **21**, 035117 (2009).
 - [30] S. Sengupta, S. Karmakar, C. Dasgupta, and S. Sastry, Breakdown of the Stokes-Einstein relation in two, three, and four dimensions, *J. Chem. Phys.* **138**, 12A548 (2013).
 - [31] R. S. Hoy and K. A. Interiano-Alberto, Efficient d -dimensional molecular dynamics simulations for studies of the glass-jamming transition, *Phys. Rev. E* **105**, 055305 (2022).
 - [32] H. J. C. Berendsen, J. P. M. Postma, W. F. van Gunsteren, A. DiNola, and J. R. Haak, Molecular dynamics with coupling to an external bath, *J. Chem. Phys.* **81**, 3684 (1984).
 - [33] https://en.wikipedia.org/wiki/Gegenbauer_polynomials.

- [34] J. Russo and H. Tanaka, Crystal nucleation as the ordering of multiple order parameters, *J. Chem. Phys.* **145**, 211801 (2016).
- [35] K. E. Blow, D. Quigley, and G. C. Sosso, The seven deadly sins: When computing crystal nucleation rates, the devil is in the details, *J. Chem. Phys.* **155**, 040901 (2021).
- [36] T. Schilling, H. J. Schöpe, M. Oettel, G. Opletal, and I. Snook, Precursor-mediated crystallization process in suspensions of hard spheres, *Phys. Rev. Lett.* **105**, 025701 (2010).
- [37] J. Russo and H. Tanaka, The microscopic pathway to crystallization in supercooled liquids, *Sci. Rep.* **2**, 505 (2012).
- [38] S. Li, Concise formulas for the area and volume of a hyperspherical cap, *Asian J. Math. Stat.* **4**, 66 (2011).
- [39] J. W. P. Schmelzer, A. S. Abyzov, V. M. Fokin, C. Schick, and E. D. Zanotto, Crystallization of glass-forming liquids: Maxima of nucleation, growth, and overall crystallization rates, *J. Non-Cryst. Solids* **429**, 24 (2015).
- [40] S. Toxvaerd, The role of local bond-order at crystallization in a simple supercooled liquid, *Eur. Phys. J. B* **93**, 202 (2020).
- [41] S. Torquato and F. H. Stillinger, New conjectural lower bounds on the optimal density of sphere packings, *Exp. Math.* **15**, 307 (2006).
- [42] L. Lue, M. Bishop, and P. A. Whitlock, Molecular dynamics study of six-dimensional hard hypersphere crystals, *J. Chem. Phys.* **155**, 144502 (2021).
- [43] Note that Ref. [44] showed that rigorously identifying separate roles for the repulsive and attractive forces in comparing the behavior of systems interacting via different potentials sharing a common functional form is impossible.
- [44] L. Bøhling, A. A. Veldhorst, T. S. Ingebrigtsen, N. P. Bailey, J. S. Hansen, S. Toxvaerd, T. B. Schrøder, and J. C. Dyre, Do the repulsive and attractive pair forces play separate roles for the physics of liquids? *J. Phys.: Condens. Matter* **25**, 032101 (2013).
- [45] Here the $E_{\text{pair}}^{\text{liq}}$ values for the LJ systems were determined by averaging E_{pair} over the time windows of length $5 \times 10^3 \tau$ immediately preceding the onset of crystallization [Fig. 1(a)]. The $E_{\text{pair}}^{\text{cryst}}$ values for all systems and the $E_{\text{pair}}^{\text{liq}}$ values for WCA systems were determined by averaging E_{pair} over the last $10^4 \tau$ of the runs used to generate the data shown in Fig. 6, i.e., over the same time windows used to calculate the averaged $P[q_6(i, j)]$ and $g(r)$.
- [46] The opposite trend was reported in 3D LJ/WCA systems, apparently because 3D WCA crystals have less lengthy low- q_6 tails; see Figs. 3 and 4 of Ref. [26].
- [47] J. D. Eaves and D. R. Reichman, Spatial dimension and the dynamics of supercooled liquids, *Proc. Natl. Acad. Sci. USA* **106**, 15171 (2009).
- [48] B. Charbonneau, P. Charbonneau, Y. Jin, G. Parisi, and F. Zamponi, Dimensional dependence of the Stokes–Einstein relation and its violation, *J. Chem. Phys.* **139**, 164502 (2013).
- [49] W. Kob and H. C. Andersen, Testing mode-coupling theory for a supercooled binary Lennard-Jones mixture. I. The van Hove correlation function, *Phys. Rev. E* **51**, 4626 (1995).
- [50] W. Kob, C. Donati, S. J. Plimpton, P. H. Poole, and S. C. Glotzer, Dynamical heterogeneities in a supercooled Lennard-Jones liquid, *Phys. Rev. Lett.* **79**, 2827 (1997).
- [51] C. Donati, J. F. Douglas, W. Kob, S. J. Plimpton, P. H. Poole, and S. C. Glotzer, Stringlike cooperative motion in a supercooled liquid, *Phys. Rev. Lett.* **80**, 2338 (1998).